Laboratory Investigation (2005) 85, 664–674

www.laboratoryinvestigation.org

Karyotypic imbalances and differential gene expressions in the acquired doxorubicin resistance of hepatocellular carcinoma cells

Elizabeth Pang[1], Ying Hu[1], Kathy Y-Y Chan[2], Paul B-S Lai[3], Jeremy A Squire[4], Pascale F Macgregor[5], Ben Beheshti[4], Monique Albert[5], Thomas W-T Leung[6] and Nathalie Wong[2]

[1]*Department of Clinical Oncology, Sir YK Pao Centre for Cancer, The Chinese University of Hong Kong, Shatin, NT, Hong Kong SAR, China;* [2]*Department of Anatomical and Cellular Pathology, Sir YK Pao Centre for Cancer, The Chinese University of Hong Kong, Shatin, NT, Hong Kong SAR, China;* [3]*Department of Surgery, Sir YK Pao Centre for Cancer, The Chinese University of Hong Kong, Shatin, NT, Hong Kong SAR, China;* [4]*Departments of Medical Biophysics and Laboratory Medicine and Pathobiology, University of Toronto, Toronto, Ontario, Canada M5G 2L9;* [5]*Microarray Centre, Clinical Genomics Centre, University Health Network, Toronto, Ontario, Canada M5G 2C4 and* [6]*Oncology Centre, Hong Kong Sanatorium & Hospital, Hong Kong SAR, China*

Administration of doxorubicin has been shown to prolong survival of patients with hepatocellular carcinoma (HCC). However, treatment regimen is often complicated by the emergence of drug resistance. The goal of our study is to enhance our understanding on the genetic changes that confer cellular chemoresistance to doxorubicin. To model this insensitive response, we established five doxorubicin-resistant (DOR) sublines through repeated exposure of escalating doses of doxorubicin to HCC cell lines (HKCI-2, -3, -4, -C1 and -C2). The DOR sublines developed displayed an average ~17-fold higher IC_{50} value than their sensitive parental cell lines. The resistant phenotype displayed was investigated by the genome-wide analyses of comparative genomic hybridization (CGH) and complementary DNA microarray for the affected genomic anomalies and deregulated genes expressed, respectively. Over-representations of regional chr. 7q11–q21, 8q22–q23 and 10p13–pter were indicated in the DOR sublines from CGH analysis. Of particular interest was the finding of amplicon augmentations from regional or whole chromosome gains during the clonal expansion of resistant sublines. Most notably, recurring amplicon 7q11.2–q21 identified coincided with the location of the multi-drug-resistant gene, *MDR1*. The potential involvement of *MDR1* was examined by quantitative reverse transcription-polymerase chain reaction RT-PCR (qRT-PCR), which indicated an upregulation in all DOR sublines ($P = 0.015$). Consistent overexpression of the translated *MDR1* gene, P-glycoprotein, in all five DOR sublines was further confirmed in Western blot analysis. Two distinct cluster dendrograms were achieved between the DOR sublines and their sensitive parental counterparts in expression profiling. Within the doxorubicin-resistant group, distinct features of candidate genes overexpressions including ABC transporting proteins, solute carriers and *TOP2A* were suggested. Further assessment of *TOP2A* messenger RNA levels by qRT-PCR confirmed array findings and pinpointed to a common up-regulation of *TOP2A* in DOR sublines. Our present study highlighted areas of genomic imbalances and candidate genes in the acquired doxorubicin-resistance behavior of HCC cells.
Laboratory Investigation (2005) **85,** 664–674, advance online publication, 14 March 2005; doi:10.1038/labinvest.3700254

Keywords: hepatocellular carcinoma; doxorubicin-resistant sublines; CGH; 7q21; array; MDR1; TOP2A

Doxorubicin and analogues are widely used first-line chemotherapeutic agents for patients with advanced hepatocellular carcinoma (HCC). Although doxorubicin has been shown to prolong patient survival, the frequent occurrence of drug resistance either at the onset or during the course of treatment has rendered the benefit of this drug only modest. Indeed, intrinsic and acquired drug resistances represent major obstacles in the successful treatment of many solid tumors. Molecular investigations on various human malignancies have

Correspondence: Dr N Wong, DPhil, Department of Anatomical and Cellular Pathology, The Chinese University of Hong Kong, Prince of Wales Hospital, Shatin, NT, Hong Kong, China.
E-mail: natwong@cuhk.edu.hk
Received 3 September 2004; revised and accepted 11 January 2005; published online 14 March 2005

implicated regions of genomic aberrations and changes in gene expression in relation to drug insensitivity.[1–4] However in HCC, although molecular studies have highlighted recurring sites of genetic alterations,[5–7] information on genes associated with drug resistance remained minimal.

Several multidrug resistance studies have employed the technique of comparative genomic hybridization (CGH) to characterize the genomic changes associated with chemoresistance. Regional gain of 1q21–q25 has been shown to correlate with resistance to aggressive treatment in progressive neuroblastomas.[2] In ovarian cancers, gain of 1q and 13q was likely related to cisplatin resistance.[3] The role of chromosome breakage in gene amplification has also been implicated by the presence of nonrandom karyotypic anomalies near the *MRP* locus in doxorubicin-resistant human fibrosarcoma cell line.[4] Advances in global expression profiling using the microarray technology has further enabled the identifications of candidate genes in the acquired resistance to anticancer drugs in gastric cancer cells[8] and the indication of a set of novel targets in association with cisplatin resistance in lung cancer cells.[9]

In vitro studies on cell lines have provided a vital approach for characterizing biological mechanisms that mediated the phenomenon of multidrug resistance. Here, we describe the establishment of five doxorubicin-resistant HCC cell lines by the continuous exposure of doxorubicin to our in-housed established series of HKCI cell lines.[10–12] In order to ascertain molecular changes by which drug resistance develops, a comprehensive evaluation on the relationships between chemoinsensitivity and consensus regions of DNA copy number and changes in genes expression have been performed by utilizing the techniques of CGH and microarray profiling, respectively.

Materials and methods

Doxorubicin-Resistant Sublines

The HKCI series of cell lines was established from the tumorous liver of patients who underwent curative surgery for HCC at the Prince of Wales Hospital, Hong Kong.[10–11] Five HCC cell lines (HKCI-2, -3, -4, -C1 and -C2) were established, three of which HKCI-2, -3, -4 have been previously described.[10,11] Using the same methodology described,[10,11] we have newly established an additional two cell lines (HKCI-C1 and -C2). Cell lines were derived from patients with differing viral hepatitis status. Two patients were seropositive for the hepatitis B virus surface antigen (HBsAg) (HKCI-3 and -4), two were seropositive for the antibody to hepatitis C (anti-HCV) (HKCI-C1 and -C2) and one patient was seronegative for both anti-HCV and HBsAg (HKCI-2). The viral status in the established cell lines was examined by the nested PCR and nested RT-PCR for the presence of HBV core/precore region and HCV for the 5′-nontranslated conserved region respectively. While the viral carriage for HBV was suggested in HKCI-4, the maintenance of neither HCV nor HBV was indicated in the remaining cell lines.

The HKCI cell lines were cultured in RPMI 1640 glutamax medium supplemented with 10% fetal bovine serum, 100 IU/ml streptomycin, 10 ng/ml selenium, 10 μg/ml transferring, and 10 μg/ml insulin. Cells, commencing at passage 25, were maintained, subcultured and chronically exposed to escalating doses of doxorubicin, starting at 0.02 μM concentration. On average, cells appeared to adapt to the cultural environment between 2 and 3 months. The selection process was performed over a period of 1 year that spanned approximately 20–25 passages.

Cytotoxic Assay

The degree of resistance to doxorubicin was determined by the modified MTT [3-(4,5-dimethythiazol-2-yl)-2,5-diphenoyltetrazolium bromide] assay. Briefly, logarithmically growing cells were harvested, counted and seeded into 96-well plates at predetermined seeding densities of $2–4 \times 10^3$ per well. These cells were incubated at 37°C for 24 h prior to the addition of sequential dilutions of doxorubicin (Pharmaceutical Laboratories, Unterach, Austria) ranging from 0 to 345 μM. Cells exposed in culture medium alone served as an experimental control. After 72 h incubation, the drug was replaced with MTT working solution at 1 mg/ml in PBS (Sigma), and incubated for a further 4 h at 37°C. The absorbance of colorimetric product formed was read at 570 nm with a microplate reader (Tecan Spectra, Austria Gmbh). The determination of IC_{50} value was performed by the linear regression analysis using the PRIZM software, version 3. An IC_{50} value was defined as the concentration of drugs that inhibited cell growth by 50% compared with experimental control.

Comparative Genomic Hybridization

High molecular weight DNA extracted from the parental cell lines and DOR sublines were subjected to CGH accordingly to the method previously described.[7] Briefly, DOR and parental DNAs were nick labeled with biotin-16-dUTP (Roche Diagnostics, Manheim Germany) and DIG-11-dUTP (Roche Diagnostics), respectively prior to hybridization onto normal metaphases for 2 days at 37°C in a humid chamber. Following posthybridization washes, biotin signals were detected through avidin conjugated fluorescein isothiocyanate (FITC) antibodies (Sigma, St Louis, MO, USA), and DIG-labeled DNA visualized using antibodies conjugated with tetramethylrhodamine isothiocyanate (TRITC)

(Sigma). Hybridized metaphases counterstained with 4′,6-diamidino-2-phenylindole (DAPI) were captured with a cooled CCD camera mounted on a Leitz DM RB (Leica) fluorescence microscope. Three-band pass filters (DAPI, FITC and TRITC) arranged in an automated filter-wheel were employed for image acquisition. The CGH software ver3.1 on Cytovision (Applied Imaging Ltd., Sunderland, UK) was used for digital image analysis of 8–12 selected metaphases. Thresholds for gains and losses were defined as the theoretical value of 1.25 and 0.75, respectively, and high-level gains when ratios exceeded 1.5.

Microarray Analysis

Total RNA from parental and resistant sublines was extracted using TRIZOL reagent (Invitrogen, Carlsbad, CA, USA). The expression array experiments were carried out according to the method of UHN Microarray Centre, Toronto, Canada (http://www.uhnres.utoronto.ca/services/microarray/protocols/). Briefly, 10 μg of total cellular RNA were reverse-transcribed by AncT messenger RNA (mRNA) primer using Superscript II reverse transcriptase (Invitrogen). Following fluorescence labeling of the transcribed complementary DNAs (cDNAs) with Cy5-dCTP or Cy3-dCTP, the cDNAs were combined with calf thymus DNA, poly(dA), and yeast tRNA in Dighyb buffer (Roche Diagnostics) prior to hybridization onto cDNA microarray slides (Ontario Cancer Institute, Canada). The 19 K EST microarray contains sequence-verified human genes and EST sequences mapped to National Center for Biotechnology Information's UniGene database. Hybridization took place in a dark chamber at 37°C for 16 h. Posthybridization washes were carried out in 1 × SCC/0.1% SDS at 50°C for three times at 10 min each, and gentle rinsing in 1 × SSC twice for 1–2 min each. The slides were then scanned with ScanArray 5000 analysis system (GSI Lumonics, Packard BioScience, Pangbourne, UK) using emission and absorption wavelengths for Cy5 and Cy3. Raw images acquired were analyzed and quantified by the GenePix Pro 4.0 (Axon, Union City, CA, USA). The raw data obtained from GenePix were normalized by custom software Normalise Suite v1.56.[12] Array experiment was carried out twice with a dye swap in the second experiment. The array data set was subjected to hierarchical clustering by the Cluster software and graphical visualization using the Treeview software.[13] The significant genes between drug-resistant and -sensitive subgroups were selected by a permutation *t-test* using the Significant for Microarray Analysis software (SAM).[14]

Quantitative RT-PCR

First-strand cDNA was prepared from total cellular RNA using random hexanucleotide primer and MultiScribe reverse transcriptase (Perkin-Elmer Applied Biosystems, Foster City, CA, USA). Quantitative PCR experiments were performed using SYBR Green PCR Core reagents kit (Perkin-Elmer Applied Biosystems). PCR amplification was performed in a 96-well optical tray, each well containing 50 μl reaction mixture that consisted 200 nM each primer, 0.025 U/μL of Ampli-Taq Gold Polymerase, 200 μM each of dATP, dCTP, and dGTP, 400 μM dUTP, and 5.5 mM $MgCl_2$. Primers were designed intron spanning based on the sequence data obtained from the NCBI database by the Primer3 software. The 5′ and 3′ primer pairs designed for *MDR1* were 5′-TGCTCA GACAGGATGTGAGTTG-3′ and 5′-TAGCCCCTTT AACTTGAGCAGC-3′ respectively, and for *TOP2A* were 5′-TTCTTGATATGCCCCTTTGG-3′ and 5′-GCTTCAACAGCCTCCAATTC-3′ respectively. The thermal cycling conditions consisted 10 min 95°C, followed by 40 cycles of 95°C for 15 s and 60°C for 1 min. The emission intensity from SYBR green binding to double-stranded DNA was detected by the iCycler detection system (BioRad Laboratories, Hercules, CA, USA). Threshold cycles were averaged from triplicate reactions and the expression in the cell lines was determined as ratio relative to the mean derived from three normal human liver tissues. To adjust for variations in starting template, the gene expression was normalized with an internal reference gene (GAPDH).

Western Blotting

Soluble protein extracts were prepared from PBS washed cells of parental HCC cells and DOR sublines. Cells at 2.5×10^6 were lysed in buffer containing 50 mM Tris-HCl (pH 8.0), 150 mM NaCl, 1% Triton X-100 and Complete™ protease inhibitors (Roche Molecular Biochemicals, Germany). The sonicated mixture in ice-water bath was left for 20 min, prior to centrifugation at 14 000*g* for 30 min at 4°C. Protein concentration in the cleared lysate supernatant was quantitated by the Bradford assay (BioRad Laboratories). An amount of 20 μg of total protein from each sample was separated by 10% SDS-PAGE and transferred to nitrocellulose membranes. Prior to the addition of primary antibody, nonspecific bindings were minimized by blocking with 5% skimmed milk in Tris-buffered saline at room temperature for 1 h. Primary antibody of *MDR1* gene product, P-glycoprotein (P-gp), at 1:500 dilution (Alexis Biochemicals, San Diego, CA, USA) or β-tubulin at 1:500 dilution (Santa Cruz Biotechnology Inc., Santa Cruz, CA, USA) was then added to the membranes and allowed to incubate overnight at 4°C. The membranes were then further incubated for 2 h with a secondary antibody conjugated to horseradish peroxidase (anti-mouse IgG-HRP at 1:1000; Sigma). The protein bands were finally visualized using an enhanced chemiluminescence detection kit (Amersham).

Statistical Analysis

Differences in IC_{50} values between parental cells and DOR sublines, and between parental cells at passages 25 and 50 were evaluated by a paired nonparametric analysis using the Wilcoxon signed rank test. The overall genomic instability as suggested from the CGH derived copy number aberrations, including gains and losses, in parental cells and DOR sublines were compared by the two-tailed unpaired Student's *t*-test. Individual chromosomal copy changes were compared by the nonparametric χ^2-test. Pearson's test was employed to assess the relationship between the expression levels of *MDR1* and *TOP2A* in relation to the degree of drug resistance as represented by the IC_{50} value. All analysis was performed with SPSS for Windows 10.0 software (SPSS Inc., Chicago, IL, USA) and the significance level was considered when *P*-value was less than 0.05.

Results

Doxorubicin-Resistant Sublines

The changes in chemoresistance in parental and DOR cell lines were determined by measuring the drug effect on cell proliferation using the MTT assay. The IC_{50} values determined on the DOR lines ranged from 10.0 to 38.8 μM (median 27.5 μM), while the corresponding parental cells displayed values that ranged from 0.4 to 3.5 μM (median 1.6 μM). The comparative range determined on DOR sublines and parental cells indicated considerable resistance to doxorubicin in the all five DOR sublines developed ($P=0.043$). An example on the altered doxorubicin tolerance in HKCI-C1-DOR subline is shown in Figure 1.

The DOR sublines were developed from parental cell lines, at passage 25, through the continuous exposure of escalating doses of doxorubicin. The selection process for resistant subclone took more than 12 months that spanned an average of 20–25 passages. To exclude the possible changes in doxorubicin tolerance being a result of prolonged *in vitro* culture, we have also compared the IC_{50} values derived at passage 25 and 50 of the parental cells. No significant differences can be concluded from the IC_{50} values between the two passages ($P>0.05$). Nevertheless, despite a similar drug-sensitive phenotype being suggested between the two passages, for the purpose of assessment in the present study, we have employed the IC_{50} values at passage 50 as a reference point for comparison with DOR sublines. Figure 2 shows the IC_{50} values derived from passages 25 and 50 of the parental HKCI cell lines, and those of the derived DOR sublines.

Genomic Imbalances

Genetic changes in sensitive parental cell lines at passages 25 and 50 were also examined to exclude karyotypic changes that might have been potentially acquired during *in vitro* cultivation. CGH profiles determined suggested the overall copy number aberrations, whether gains or losses, was similar between the two passages ($P>0.05$). No significant changes were also indicated at the individual chromosome level ($P>0.05$).

Similar to the cytotoxic study, we have also employed the CGH profile of the parental cell lines at passage 50 in comparison with the corresponding DOR sublines. A comparative list of chromosomal copy number deviations determined is presented in Table 1. Evaluation of copy number aberrations between each parental line and corresponding DOR subline did not suggest differences in chromosomal instability ($P>0.05$). A number of genetic imbalances including gains of 1q, 7, 19 and 20, and losses

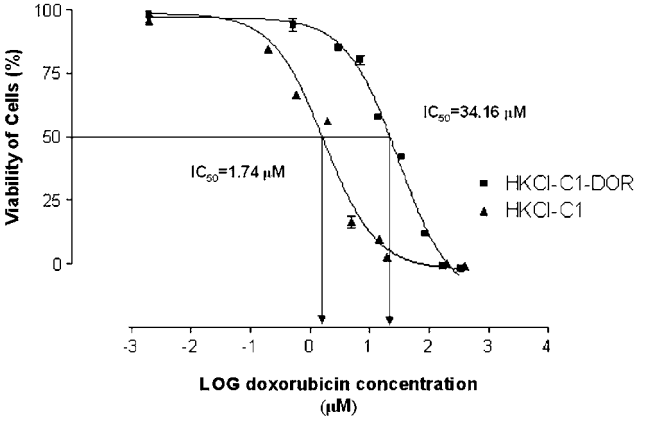

Figure 1 Development of doxorubicin-resistant DOR subline. The cell viability in the presence of doxorubicin was determined by the MTT assay. Comparison of IC_{50} values determined in HKCI-C1 and HKCI-C1-DOR suggested an increment in the resistance to doxorubicin by almost 20-fold in the DOR subline.

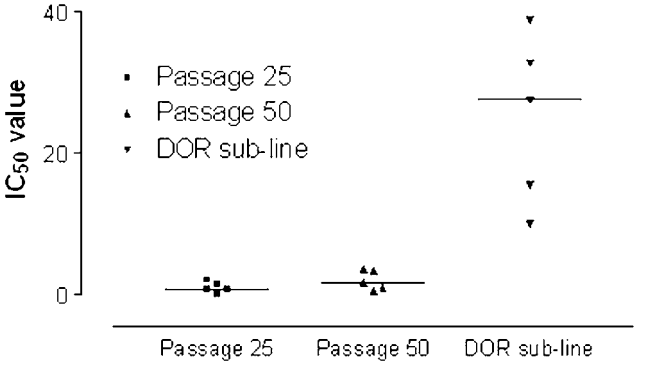

Figure 2 IC_{50} values determined in the parental cell lines at passages 25 and 50, and derived DOR sublines. Similar IC_{50} values towards doxorubicin were suggested at passages 25 and 50 of parental cells. DOR sublines derived, on the other hand, displayed consistent increments in IC_{50} values, which suggested an acquired drug insensitivity phenotype arising from prolonged doxorubicin exposure.

Table 1 Genomic imbalances in parental cell lines and corresponding DOR sublines

	Parental cell line	*DOR subline*
HKCI-2	+1q21–q31, +5, +7, +8q22–qter, +10p, +12, −13q, −15q22–qter, +16, +19, +20, +X	+1q21–q25, −4q, **+7q11.2–q22**, +7q31–qter, −9p, −9q22–qter, −10q24–qter, +12q12–qter, −13q21, +14q, +19, +20, **+X**
HKCI-3	+1q, −4q22–qter, +5p, −6q13–qter, +7, −9pter–p21, **+10p**, −10q, −11p12–q12, −11q14–qter, −12p, +12q12–q22, +13q, +14q11.2–q13, +15q, **+19**, −21, **+**22q12, −22q13, −Y, +X	+4p, −4q22–qter, −6q13–qter, +7, +8q22–qter, **+10pter–p14**, +10p11.2, −10q21, −10q24–qter, +11q23–qter, +15q, +16, −19q, +20, **+Xp22.2–p21**
HKCI-4	−1p35–p31, +1q21–q25, +3q, −4p14–qter, **+5p**, +6p, −6q12–q13, **+7**, +8q22, **+8q23–qter**, −10q, +11p, **+11q13**, +12, −13q21–q22, +15q11.2–q–21, −16pter–p12, +17, +19, +20, −Y	+1pter–p36.1, +1q21, −4p12–q31.3, **+5p**, −5q23, **+**6p, −6q12–q22, **+**7p, **+7p11.2–q21**, +7q31–qter, +8q22–qter, +9q34, +10p, +11q13, −11q14–qter, +12pter–q14, **+12q15–q22**, −13q, +15q14–q21, +19p, **+19q13.3**, +20
HKCI-C1	+5q, −9p, +9q34, +11q, −13q, +16p, +19, **+20**	+8q22–qter, +10p, −13q, +18p11.2, +19, +20
HKCI-C2	+1p31–qter, −4q, −5, +7, +9p, +11q12–q22, +12p, +16q, +17q, +19, +20, +X	+1q21, +2p22–q33, +3q24–q25, −3q27–qter, −4q26–qter, −5, +6q22, +7, −8pter–p21, +8q11.2–q23, +9p23–p12, +20

CGH analysis indicated copy gains and losses in the sensitive parental cell lines and doxorubicin-resistant DOR sublines derived. Bold type indicates amplifications, and additional genomic changes in the DOR sublines that differed from the parental cell lines are underlined.

of 4q and 13q were common in both groups, although recurring regional over-representations of 8q22–q23 and 10p13–pter (3/5 DOR cell lines each) and 7q11.2–q21 (2/5 DOR cell lines) were suggested in the resistant sublines compared to the parental counterparts.

It was also remarkable to find the augmentation of new chromosomal events from pre-existing copy gain. In HKCI-2 and -4, copy gain of whole chromosome 7 detected in the parental lines was found to have intensified at regional 7q11.2–q22 and 7p11.2–q21, respectively, in the DOR sublines (Table 1). This phenomenon was also observed on chromosomes 10p, 12, 19 and X. Additional amplicons at 12q15–q22 and 19q13.3 from whole chromosome gain of 12 and 19 in HKCI-4-DOR were indicated, while in HKCI-3-DOR intensification of 10p14–pter and Xp22.2–p21 were shown from 10p and X copy gain. Example on the development of regional amplicon on chromosome 7 in the DOR subline of HKCI-2 is shown in Figure 3.

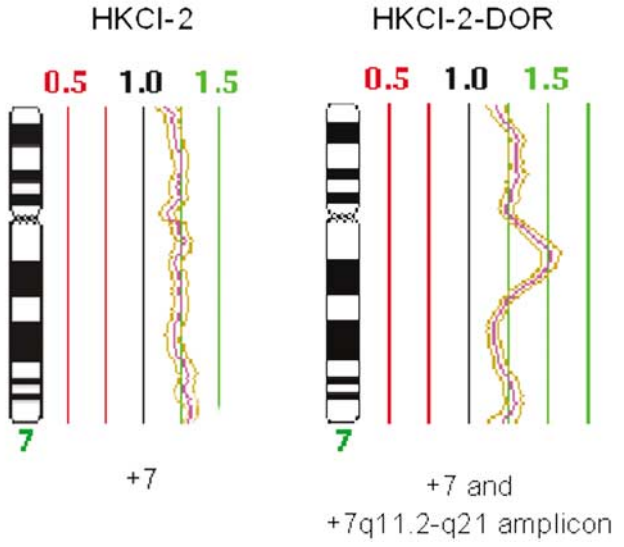

Figure 3 CGH profile of chromosome 7 in the parental HKCI-2 and corresponding HKCI-2-DOR subline. CGH analysis on the parental HKCI-2 revealed whole chromosome gain of chromosome 7, while in HKCI-2-DOR an augmentation of 7q21–q22 amplicon was indicated in addition to the chromosome 7 copy gain. The mean ratio profile of 8–12 analyzed chromosomes (pink line) is depicted along with the 95% confidence interval (gold lines).

Array Profiling

The expression profiles determined in doxorubicin-sensitive parental cell lines at passage 50 were compared to the resistant DOR sublines and analyzed by web-available software ('Cluster' and 'TreeView'). Before the clustering algorithm was applied, the fluorescence ratio for each spot was first log-transformed (log 2); thereafter the data for each sample were median-centered to remove experimental biases. By hierarchical clustering in an unsupervised manner, 10 HCC cell lines were classified into two distinct dendrogram that coincided with their drug sensitivity and resistance phenotypes (Figure 4). The five DOR sublines clustered independently from the sensitive parental cell lines suggesting distinct features associated with the acquired doxorubicin-resistance phenomenon. The microarray data sets were further subjected to significance analysis of microarrays (SAM) to highlight candidate genes induced from prolonged doxorubicin treatment. Differentially expressed candidates identified from SAM were predominantly upregulated genes and those with a median fold gain of two-fold or more are listed in Table 2. These deregulated genes belonged to a broad range of functional pathways that included

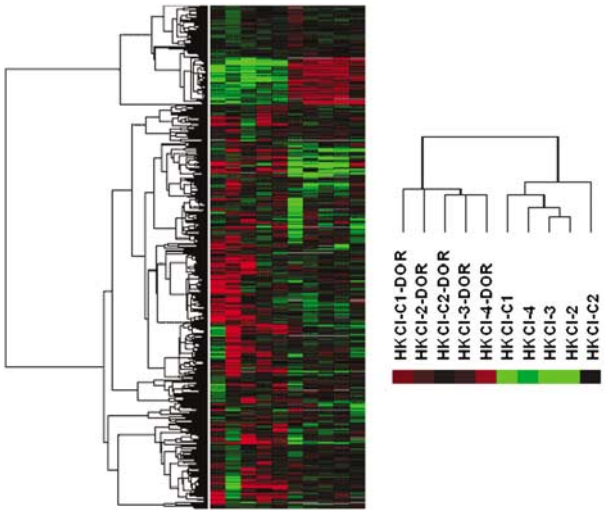

Figure 4 Hierarchical clustering on expression profiles of parental cell lines and DOR sublines. Global expression array analysis was performed to evaluate the differentially expressed genes associated with the acquired drug resistance phenomenon observed in the DOR sublines. Expression profiles of 10 HCC cell lines of differing tolerance to doxorubicin were found to classify into two distinct dendrograms. From unsupervised hierarchical clustering, five parental cell lines (HKCI-2, -3, -4, -C1 and -C2) clustered independently from the five corresponding drug-resistant DOR sublines, suggesting distinct features in conferring the antiapoptotic effect towards doxorubicin.

cellular membrane transports, intracellular trafficking, metabolic regulators and the control of cell cycle.

Candidate Gene Expression

The identification of overlapping regional amplifications at chromosome 7q21–q22 in resistant sublines has prompted our speculation for the involvement of the *MDR1* gene (*multidrug resistance 1*; member of the superfamily of ATP-binding cassette (ABC) transporters) from within the region. Indeed, array analysis has suggested overexpressions of ABC transporters in the DOR sublines (Table 2). Of interest was also the finding in the DOR sublines a recurring up-regulation of *TOP2A* (*Topoisomerase II alpha*), a well-known target for the anticancer effect of doxorubicin. The *TOP2A* deregulation was suggested in all DOR sublines, except in HKCI-2-DOR. Further analysis by quantitative reverse transcription-polymerase chain reaction RT-PCR (qRT-PCR) confirmed an elevated expression of *MDR1* that ranged from 4.2- to 44.2-fold in the DOR sublines when compared to the basal expression levels in parental lines ($P=0.015$). Western blot analysis for the translated *MDR1* gene product, P-gp substantiated a consistent P-gp overexpression in all five DOR sublines compared to only low or negligible levels found in the parental cells (Figure 6).

An increased *TOP2A* expression in the four DOR sublines as indicated from array analysis (HKCI-3, -4, -C1 and -C2-DOR) was also verified from qRT-PCR study, which further pinpointed to an increment of 1.6–8.9-fold in the resistant sublines compared to the sensitive parental cells. A positive correlation between *TOP2A* expression and an increased drug resistant phenotype as represented by the IC_{50} values was suggested from our study, although statistical correlation did not reach significant level ($P=0.08$). Figure 5 highlights the *MDR1* and *TOP2A* overexpression in DOR sublines compared to the parental cell lines.

Discussion

Development of acquired doxorubicin resistance is a common phenomenon in HCC. While it is known that both intrinsic and acquired resistance of cancer cells can limit the effectiveness of systemic chemotherapy, the genetic changes underlying such drug resistance behavior in HCC remained not well understood. To model the acquired changes by which drug resistance develops, we have established five doxorubicin resistant sublines through prolonged exposure of escalating doses of doxorubicin to human HCC cell lines. Comparative analyses in resistant sublines and sensitive parental cells have yielded changes in gene expression levels and affected chromosomal loci.

Identification of intrinsic genomic changes involved in the antiapoptotic effect towards doxorubicin would potentially provide areas for further investigations on the causal genes involved. Here, we have employed the technique of CGH for the genomewide characterization of genetic imbalances present. Comparison of genomic anomalies in doxorubicin-resistant cell lines and the sensitive counterparts by CGH did not suggest differences in the chromosomal instability ($P>0.05$). While the overall copy number aberrations did not seem to play a role in conferring the resistance phenotype, specific regional over-representations of 7q21–q22, 8q22–qter and 10p13–pter were suggested in the DOR cell lines. It is well recognized that cells with genetic alterations possessing a growth or survival advantage would lead to clonal expansion. Moreover, a number of these alterations described were mediated by copy number gains, particularly regional DNA amplifications. Here, the detection of amplicons 7q11.2–q21, 10p14–pter, 12q12–q22, 19q13.3 and Xp22.2–p21 in the DOR sublines may hold biological relevance in the acquired drug resistance phenotype observed.

The differential gene expression changes involved in the acquired doxorubicin-resistant phenotype were investigated by comparing the global gene expression patterns between resistant and sensitive cells using microarray. In unsupervised hierarchical clustering of array data, we observed an indepen-

Table 2 SAM analysis on array data sets indicated predominantly upregulated genes in the acquired doxorubicin resistance phenotype

UniGene ID	*Gene name*	*Symbol*	*Function*
Hs.434433	Golgi autoantigen	*GOLGA4*	Transportation of proteins and lipids in the secretory pathway
Hs.102929	NCK interacting protein with SH3 domain	*NCKIPSD*	Signal transduction and stress fiber formation
Hs.351342	Ras suppressor protein 1	*RSU1*	Ras signal transduction pathway and growth inhibition
Hs.19383	Angiotensinogen proteinase inhibitor	*AGT*	Maintenance of blood pressure
Hs.174193	Zinc-finger protein 335	*ZNF335*	Enhances transcriptional activation
Hs.171695	Dual specificity phosphatase 1	*DUSP1*	Negative regulator of cellular proliferation in response to environmental stress
Hs.126550	Vacuolar protein sorting 4B	*VPS4B*	Intracellular protein trafficking
Hs.271980	Mitogen-activated protein kinase 6	*MAPK6*	Extracellular signaling and integral point for multibiochemical signals
Hs.29379	GPP34-related protein	*GPP34R*	Regulatory role in Golgi trafficking
Hs.352018	Transporter 1, ATP-binding cassette	*MDR/TAP1*	ABC transporter associated with cellular membrane trafficking and multidrug resistance
Hs.156346	Topoisomerase (DNA) II, alpha	*TOP2A*	Target of several anticancer agents and associated with drug resistance development
Hs.170359	Interleukin 16	*IL16*	Pleiotropic cytokine that functions as a chemoattractant, cell cycle controller and modulator of T-cell activation
Hs.515717	FUS interacting protein	*FUSIP1*	A serine–arginine protein involve in constitutive and regulation of RNA splicing
Hs.5344	Adaptor-related protein complex 1	*AP1G1*	Transportation of ligand–receptor complexes from plasma membrane or trans-Golgi network to lysosomes
Hs.10842	RAN, member of RAS family	*RAN*	Control of DNA synthesis and cell cycle progression
Hs.170622	Cofilin 1	*CFL1*	Translocation of actin–cofilin complex from cytoplasm to nucleus
Hs.20447	p21(CDKN1A)-activated kinase 4	*PAK4*	Mediator of filopodia formation and in reorganization of actin cytoskeleton
Hs.300774	Fibrinogen, B beta polypeptide	*FGB*	Regulates cell adhesion and spreading, displays vasoconstrictor and chemotactic activities, and behaves as a mitogen for several cell types
Hs.76753	Endoglin	*ENG*	Trans-membrane glycoprotein belonging to the transforming growth factor beta-receptor complex
Hs.32018	SNAP-associated protein	*SNAPAP*	Synaptic vesicle docking and fusion
Hs.280226	Apolipoprotein B	*APOB*	Main apolipoprotein of chylomicrons and low-density lipoproteins
Hs.181243	Activating transcription factor 4	*ATF4*	Protein–protein interactions and DNA binding
Hs.371233	Male-specific lethal 3-like 1	*MSL3L1*	Chromatin remodeling and transcriptional regulation
Hs.242947	Diacylglycerol kinase	*DGKI*	Production of phosphatidic acid in the retina or in recessive forms of retinal degeneration
Hs.278388	Orosomucoid 2	*ORM2*	Acute phase plasma protein in immunosuppression
Hs.75431	Fibrinogen, gamma polypeptide	*FGG*	Regulates cell adhesion, spreading and behaves as a mitogen for several cell types
Hs.449863	Acetyl-coenzyme A carboxylase, alpha	*ACACA*	Catalyzes carboxylation of acetyl-CoA to malonyl-CoA in the fatty acid synthesis
Hs.416998	Mitochondrial ribosomal protein L18	*MRPL18*	Protein synthesis within the mitochondrion
Hs.132246	Solute carrier family 38	*SLC38A1*	Amino-acid transporter in nutrients uptake, chemical metabolism and detoxification
Hs.9994	Lipase, hepatic	*LIPC*	Receptor-mediated lipoprotein uptake
Hs.433488	Guanylate cyclase 1, alpha 3	*GUCY1A3*	Main receptor for nitric oxide and nitrovasodilator drugs
Hs.83126	TAF11 RNA polymerase II	*TAF11*	Coactivator in the initiation of transcription
Hs.254042	HLA-B-associated transcript 1	*BAT1*	Initiation of translation, RNA splicing, and ribosome assembly
Hs.131059	Ankyrin repeat domain 17	*ANKRD17*	Protein–protein interactions and liver development
Hs.2499	Protein kinase C-like 1	*PRKCL1*	Mediates Rho-dependent signaling pathway
Hs.133082	DEAD box polypeptide 31	*DDX31*	Cellular growth and division
Hs.406532	Ribophorin II	*RPN2*	Links high mannose oligosaccharides to asparagine residues
Hs.201671	SRY-box 13	*SOX13*	Transcriptional regulator in the regulation of embryonic development and determination of cell fate
Hs.16244	Sperm-associated antigen 5	*SPAG5*	Functional and dynamic regulation of mitotic spindles
Hs.26412	Ring finger protein 26	*RNF26*	Protein–DNA and protein–protein interactions
Hs.293636	Serine hydroxy-methyltransferase 1	*SHMT1*	Catalyzes the synthesis of methionine, thymidylate, and purines in the cytoplasm
Hs.305890	BCL2-like 1	*BCL2L1*	Anti- or pro-apoptotic regulator in a wide variety of cellular activities
Hs.439660	Ring finger protein 19	*RNF19*	E3 ubiquintin ligase
Hs.268012	Acyl-CoA synthetase	*ACSL3*	Lipid biosynthesis and fatty acid degradation

Table 2 Continued

UniGene ID	*Gene name*	*Symbol*	*Function*
Hs.356502	Ribosomal protein	*RPLP1*	Catalyzes protein synthesis, in particular at the step of elongation
Hs.75342	Malic enzyme 2, NAD(+)-dependent	*ME2*	Oxidative decarboxylation of malate to pyruvate in mitochondria
Hs.30868	Reticulon 4 receptor	*RTN4R*	Regulation of axonal regeneration and plasticity of adult central nervous system
Hs.7370	Phosphotidylinositol transfer protein	*PITPNB*	Transfer of phospholipids between membranes *in vitro*
Hs.50915	Kallikrein 5	*KLK5*	Serine protease with diverse physiological functions
Hs.439312	Phospholipid transfer protein	*PLTP*	Cholesterol metabolism
Hs.76353	Serine proteinase inhibitor	*SERPINA3*	Plasma protease inhibitor
Hs.403933	F-box only protein 32	*FBXO32*	Phosphorylation-dependent ubiquitination
Hs.446414	CD47 antigen	*CD47*	Integrin-associated membrane transporter and signal transducer
Hs.7960	DnaJ (Hsp40) homolog, member 12	*DNAJB12*	Regulates molecular chaperone activity by stimulating ATPase activity
Hs.13040	G protein-coupled receptor 86	*GPR86*	Receptor subtypes with pharmacological selectivity
Hs.439023	Serine dehydratase	*SDS*	Metabolism of serine to pyruvate and ammonia
Hs.82285	Phosphoribosylglycinamide formyltransferase	*GART*	Activity required for *de novo* purine biosynthesis
Hs.23255	Nucleoporin 155kDa	*NUP155*	Bi-directional trafficking of mRNAs and proteins between nucleus and cytoplasm
Hs.150833	Complement component 4A	*C4A*	Interactions between antigen–antibody complex
Hs.132037	Pescadillo homolog 1	*PES1*	Cell proliferation, oncogenic transformation and tumor progression
Hs.511951	ATP-binding cassette, sub-family B, member 9	*ABCB9*	ABC transporter associated with cellular membrane trafficking and multi-drug resistance
Hs.8026	Sestrin 2	*SESN2*	Regulation of cell growth, survival and cellular responses to stress conditions
Hs.274543	Mitochondrial elongation factor	*EFG1*	Maintenance of respiratory chain-oxidative phosphorylation system
Hs.356285	High-mobility group nucleosome binding domain 1	*HMGN1*	Maintenance of transcribable genes in a unique chromatin conformation

dent cluster of DOR sublines, suggesting distinct transcriptional features that underlined the phenomenon of doxorubicin resistance (Figure 4). Further permutation *t*-test analysis by SAM indicated predominantly upregulated genes in the mediation of doxorubicin resistance. The identified genes belonged to a broad range of functional pathways that included membrane transports (*MDR/TAP1*, *ABCB9*), intracellular trafficking (*VPS4B*, *CFL1*), signaling pathways (*MAPK6*, *CD47*), transcription (*TOP2A*, *ATF4*), metabolic regulations (*SLC38A1*, *EFG1*) and the control of cell cycle (*RAN*, *BCL2L1*) (Table 2).

Anthracyclines, such as doxorubicin, have been found to function through the inhibition of topoisomerase II. Resistance to topoisomerase II inhibitors can be characterized by an overexpression of *MDR1* or *TOP2A*, although decreased expression of *TOP2A* has also been suggested in the resistance of anticancer therapy.[15] Regional overlapping amplifications of 7q21–q22 identified in the DOR sublines coincided with the physical location of the *MDR1* gene at 7q21.12. Parallel expression array analysis also supported the up-regulation of ABC transporters in the intrinsic transcriptional changes leading to doxorubicin resistance. qRT-PCR confirmed an overexpression of *MDR1* gene in the resistant sublines and further pinpointed to a substantially lower *MDR1* expressions in the parental cells prior to the extended period of doxorubicin induction. In this study, we found a 4.2–44.2-fold increment of *MDR1* expression between the parental and DOR sublines. In addition, a linear correlation between the levels of *MDR1* expression and the degree of doxorubicin resistance was also indicated ($P = 0.015$). The *MDR1* gene product encodes the P-gp, which is a transmembrane glycoprotein belonging to the superfamily of ABC transporters.[16] In concordance with the RNA levels determined from qRT-PCR, Western Blot analysis substantiated an overexpression of P-gp in all DOR sublines that exceeded the basal levels found in the corresponding parental cells (Figure 6). It is believed that overexpression of P-gp confers drug-resistance via an increased cellular drug efflux from the binding of drug molecules to P-gp within the lipid bilayer cell membrane.[17] An elevated expression of P-gp has been described in the intrinsic drug-resistant behavior of colon, renal and adrenal cancers, and in some tumors that acquired drug resistance after chemotherapy.[18,19] In HCC, frequent overexpression of P-gp has been suggested in the

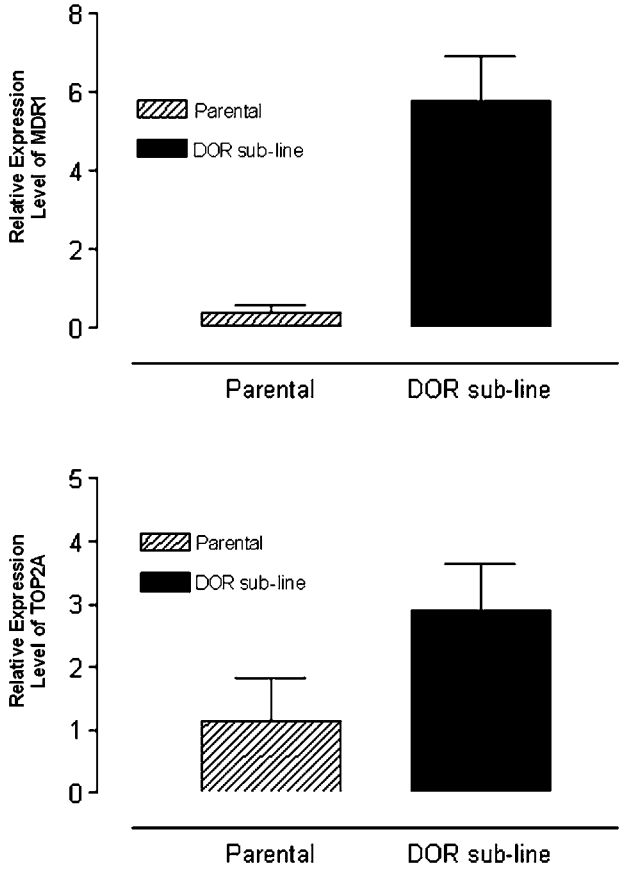

Figure 5 Relative mRNA expression levels of *MDR1* and *TOP2A* in parental cells and DOR sublines. Increased expression levels of *MDR1* and *TOP2A* were suggested in DOR sublines compared to parental cell lines. A significant increment in *MDR1* expression was further suggested in the DOR sublines ($P=0.015$). The bars highlight the means of expression levels $\pm$ SD.

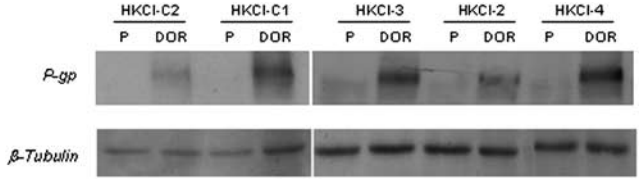

Figure 6 *MDR1* protein expression in parental HCC cells and DOR sublines. Western blot analysis on parental HCC cell lines (P) and doxorubicin-resistant sublines (DOR) indicated consistent overexpression of the translated *MDR1* gene product, P-gp, in the drug-resistant sublines compared to parental cells.

poor response to chemotherapy.[20,21] Further *in vitro* evidences have suggested that *MDR1* modulators could significantly improved the response of pediatric liver cancer cells to doxorubicin[22] and a reversal of drug resistance has been demonstrated from the delivery of anti-*MDR1* ribozymes into HCC cells.[23] Nevertheless, while the mechanism of *MDR1* have been extensively studied both *in vitro* and *in vivo*, a number of clinical trials has failed to show any important benefits in response to chemotherapy or the length of patient survival using P-gp-reversing agents.[24,25] This may in turn be suggestive of concomitant resistance mechanisms also playing a role in the chemoinsensitivity of malignant cells.

The *TOP2A* gene encodes a DNA topoisomerase, an enzyme that controls and alters the topologic states of DNA during transcription. The gene encoding this enzyme functions as the target for several anticancer chemotherapeutic agents, including doxorubicin, and a variety of mutations in this gene has been described in the development of drug resistance.[26,27] Increased expression of *TOP2A* has been suggested in tumor recurrences of colon cancer[28] and in association with poorer patients survival and the presence of metastases in malignant peripheral nerve sheath tumors.[29] In HCC, *TOP2A* overexpression appears to be related to a potentially aggressive tumor phenotype and may be indicative of tumor recurrences.[30] Here, gene expression profiling suggested an increased *TOP2A* expression to correlate with the acquired drug resistance to doxorubicin. qRT-PCR confirmed array findings and indicated an increment in *TOP2A* mRNA levels by 1.6–8.9-fold in DOR sublines relative to their sensitive counterparts. Using experimental *in vitro* models, an increased *TOP2A* expression has also been suggested in the acquired resistance to radiation and chemotherapeutic agents in small-cell lung cancer (SCLC).[31] In the same study, a five-fold increment of *TOP2A* expression was indicated in the SCLC subline when compared to the parental cells, and a role for the *TOP2A* upregulation in the resistant behavior was suggested.[31]

In this study, we described the establishment and analysis of five DOR cell lines for their genomic changes and differential genes expression that conferred an acquired resistant phenotype to doxorubicin. Clonal expansion of DOR sublines appeared to involve the modulation of DNA copy number gains, particularly 7q11.2–q21, 8q22–q23 and 10p13–pter. The regional over-representations might have signified the translation of predominantly upregulated genes detected from array analysis. Overexpression of candidate genes identified may well have conferred the growth and survival advantages to malignant hepatocytes under the selective conditions of chronic drug exposure. Our study also demonstrates that a global genomic overview can be instrumental in defining a focused approach to identifying genomic regions and highlighting genes, such as *MDR1 and TOP2A*, in the drug-resistant phenomenon of HCC cells. Nevertheless, drug resistance is thought to be mediated through multiple complimentary pathways. Indeed, many of our array-determined candidate genes have been proposed in mechanisms include enhanced drug efflux pumps, increased intracellular drug detoxification, alterations in nuclear targets, modifications of DNA repair systems, and activation of antiapoptotic pathways. It is therefore likely that a

combination of genes operates in conjunction during the development of doxorubicin resistance.

Acknowledgements

This work was supported by a RGC grant of SAR Hong Kong (Ref. No.: CUHK 4097/02M), a Direct Grant and Strategic Area Research grant from the Chinese University of Hong Kong, and in part by the Kadoorie Charitable Foundations (under the auspices of the Hong Kong Cancer Genetics Research Group).

References

1 Weber RG, Rieger J, Naumann U, *et al.* Chromosomal imbalances associated with response to chemotherapy and cytotoxic cytokines in human malignant glioma cell lines. Int J Cancer 2001;91:213–218.
2 Hirai M, Yoshida S, Kashiwagi H, *et al.* 1q23 gain is associated with progressive neuroblastoma resistant to aggressive treatment. Genes Chromosomes Cancer 1999;25:261–269.
3 Kudoh K, Takano M, Koshikawa T, *et al.* Comparative genomic hybridization for analysis of chromosomal changes in cisplatin-resistant ovarian cancer. Hum Cell 2000;13:109–116.
4 Slovak ML, Ho JP, Cole SP, *et al.* The LRP gene encoding a major vault protein associated with drug resistance maps proximal to MRP on chromosome 16: evidence that chromosome breakage plays a key role in MRP or LRP gene amplification. Cancer Res 1995;55: 4214–4219.
5 Marchio A, Meddeb M, Pineau P, *et al.* Recurrent chromosomal abnormalities in hepatocellular carcinoma detected by comparative genomic hybridization. Genes Chromosomes Cancer 1997;18:59–65.
6 Boige V, Laurent-Puig P, Fouchet P, *et al.* Concerted nonsyntenic allellic losses in hyperploid hepatocellular carcinoma as determined by a high-resolution allelotype. Cancer Res 1997;57:1986–1990.
7 Wong N, Lai P, Lee SW, *et al.* Assessment of genetic changes in hepatocellular carcinoma by comparative genomic hybridization analysis: relationship to disease stage, tumor size, and cirrhosis. Am J Pathol 1999; 154:37–43.
8 Kang HC, Kim IJ, Park JH, *et al.* Identification of genes with differential expression in acquired drug-resistant gastric cancer cells using high-density oligonucleotide microarrays. Clin Cancer Res 2004;10:272–284.
9 Whiteside MA, Chen DT, Desmond RA, *et al.* A novel time-course cDNA microarray analysis method identifies genes associated with the development of cisplatin resistance. Oncogene 2004;23:744–752.
10 Pang E, Wong N, Lai PB, *et al.* A comprehensive karyotypic analysis on a newly developed hepatocellular carcinoma cell line, HKCI-1, by spectral karyotyping and comparative genomic hybridization. Cancer Genet Cytogenet 2000;121:9–11.
11 Pang E, Wong N, Lai PB, *et al.* Consistent chromosome 10 rearrangements in four newly established human hepatocellular carcinoma cell lines. Genes Chromosomes Cancer 2002;33:150–159.
12 Beheshti B, Braude I, Marrano P, *et al.* Chromosomal localization of DNA amplifications in neuroblastoma tumors using cDNA microarray comparative genomic hybridization. Neoplasia 2003;5:53–62.
13 Eisen MB, Spellman PT, Brown PO, *et al.* Cluster analysis and display of genome wide expression patterns. Proc Natl Acad Sci USA 1998;95:14863–14868.
14 Tusher VG, Tibshirani R, Chu G. Significance analysis of microarrays applied to the ionizing radiation response. Proc Natl Acad Sci USA 2001;98:5116–5121.
15 Beck WT, Morgan SE, Mo YY, *et al.* Tumor cell resistance to DNA topoisomerase II inhibitors: new developments. Drug Resist Updat 1999;2:382–389.
16 Chen CJ, Chin JE, Ueda K, *et al.* Internal duplication and homology with bacterial transport proteins in the mdr1 (P-glycoprotein) gene from multidrug-resistant human cells. Cell 1986;47:381–389.
17 Gottesman MM, Fojo T, Bates SE. Multidrug resistance in cancer: role of ATP-dependent transporters. Nat Rev Cancer 2002;2:48–58.
18 Fojo T, Bates S. Strategies for reversing drug resistance. Oncogene 2003;22:7512–7523.
19 Gouaze V, Yu JY, Bleicher RJ, *et al.* Overexpression of glucosylceramide synthase and P-glycoprotein in cancer cells selected for resistance to natural product chemotherapy. Mol Cancer Ther 2004;3:633–639.
20 Xiao E, Hu G, Liu P, *et al.* The effect of different interventional treatment on P-Glycoprotein in different histopathological types and grades of primary hepatocellular carcinoma. J Tongji Med Univ 2000;20: 231–234.
21 Chenivesse X, Franco D, Brechot C. MDR1 (multidrug resistance) gene expression in human primary liver cancer and cirrhosis. J Hepatol 1993;18:168–172.
22 Warmann S, Gohring G, Teichmann B, *et al.* P-glycoprotein modulation improves *in vitro* chemosensitivity in malignant pediatric liver tumors. Anticancer Res 2003;23:4607–4611.
23 Huesker M, Folmer Y, Schneider M, *et al.* Reversal of drug resistance of hepatocellular carcinoma cells by adenoviral delivery of anti-MDR1 ribozymes. Hepatology 2002;36:874–884.
24 Sonneveld P, Suciu S, Weijermans P, *et al.* Cyclosporin A combined with vincristine, doxorubicin and dexamethasone (VAD) compared with VAD alone in patients with advanced refractory multiple myeloma: an EORTC-HOVON randomized phase III study (06914). Br J Haematol 2001;115:895–902.
25 Dalton WS, Crowley JJ, Salmon SS, *et al.* A phase III randomized study of oral verapamil as a chemosensitizer to reverse drug resistance in patients with refractory myeloma. A Southwest Oncology Group Study. Cancer 1995;75:815–820.
26 Okada Y, Tosaka A, Nimura Y, *et al.* Atypical multidrug resistance may be associated with catalytically active mutants of human DNA topoisomerase II alpha. Gene 2001;272:141–148.
27 Patel S, Sprung AU, Keller BA, *et al.* Identification of yeast DNA topoisomerase II mutants resistant to the antitumor drug doxorubicin: implications for the mechanisms of doxorubicin action and cytotoxicity. Mol Pharmacol 1997;52:658–666.
28 Lazaris AC, Kavantzas NG, Zorzos HS, *et al.* Markers of drug resistance in relapsing colon cancer. J Cancer Res Clin Oncol 2002;128:114–118.

29 Skotheim RI, Kallioniemi A, Bjerkhagen B, *et al.* Topoisomerase-II alpha is upregulated in malignant peripheral nerve sheath tumors and associated with clinical outcome. J Clin Oncol 2003;21:4586–4591.
30 Watanuki A, Ohwada S, Fukusato T, *et al.* Prognostic significance of DNA topoisomerase IIalpha expression in human hepatocellular carcinoma. Anticancer Res 2002;22:1113–1119.
31 Henness S, Davey MW, Harvie RM, *et al.* Fractionated irradiation of H69 small-cell lung cancer cells causes stable radiation and drug resistance with increased MRP1, MRP2, and topoisomerase IIalpha expression. Int J Radiat Oncol Biol Phys 2002;54:895–902.